

# Control of hydrogen content and fuel recycling for long pulse high performance plasma operation in EAST tokamak

Y. W. Yu<sup>1</sup>, J. S. Hu<sup>1,2</sup>, G.Z. Zuo<sup>1</sup>, Z. Sun<sup>1,3</sup>, L. Wang<sup>1</sup>, W. Xu<sup>1</sup>, J.R. Wang<sup>1</sup>, B. Cao<sup>1</sup>, W. Gao<sup>1</sup>, J.C. Xu<sup>1</sup>, J. G. Li<sup>1</sup> and the EAST Team

<sup>1</sup>*Institute of Plasma Physics, Chinese Academy of Sciences, Hefei 230031, China*

<sup>2</sup>*CAS key Laboratory of Photovoltaic and energy conservation materials, Hefei 230031, China*

<sup>3</sup>*Princeton Plasma Physics Laboratory, 100 Stellarator Road, Princeton, NJ 08540, United States of America*

E-mail: [yuyaowei@ipp.ac.cn](mailto:yuyaowei@ipp.ac.cn) and [hujs@ipp.ac.cn](mailto:hujs@ipp.ac.cn)

## Abstract

Control of fuel recycling and hydrogen content for by using various methods in Experimental Advanced Superconducting Tokamak (EAST) is studied for high-power long pulse H-mode plasma operation. The results show that long time first wall baking and discharge cleaning in EAST provides necessary clean vacuum environment with a high ultimate vacuum of  $3.6 \times 10^{-6}$  Pa and low outgassing rate of  $\sim 1.5 \times 10^{-4}$  Pa m<sup>3</sup>/s for plasma operation. In-Vessel Cryopumps (IVCP) is found to be an efficient method for particle recycling control on divertor region to decrease global recycling coefficient ( $R_{global}$ ) from  $\sim 1.0$  to  $\sim 0.8$  during Ohmic Heating (OH) plasmas, and it provides high particle exhausting rate of  $10^{20}$ -  $10^{21}$  D-atoms/s in high-power plasma operations. Long-term silicon coating (SiD<sub>4</sub>) is found to is more powerful than baking and discharge cleanings, which reduces H/(H+D) ratio gradually to a value as low as 8%, and lithium coating is more effective and more efficient than silicon coating to further reduce H/(H+D) ratio to 3%. Real-time Lithium Powder Injection (LPI) is a novel and real-time method for recycling control, which reduces  $R_{global}$  from by 0.94 to 0.82 under lithium coating wall condition. By the combination and optimization of the above methods, H-mode plasmas with low hydrogen content and low fuel recycling are achieved in EAST and extended gradually to 101 s in 2017, and recycling flux is even decreased gradually during 101 s H-mode plasmas due to increased first wall temperature and therefore increased Li-II emission. These results provide valuable references on hydrogen content and fuel recycling control for long pulse H-mode plasma of up to 400 - 1000 s with high power heating in EAST and future fusion device such as ITER.

PACS numbers: 52.40.Hf, 52.55.Fa

Keywords: fuel recycling, long pulse operation, wall conditioning, hydrogen content, EAST

## 1. Introduction

Fuel recycling is one of most important issues for high performance long pulse operation of tokamaks [1,2]. Plasma density control becomes difficult in the later phase of long pulse high power operation, because fuel recycling induced by thermal desorption from first wall surface and other in-vessel components with increasing temperature could be increased gradually. A low edge fuel recycling is necessary to obtain high performance plasmas with high confinement [3]. Moreover, a low hydrogen level,  $< 10\%$  of  $H/(H+D)$ , is a basic requirement of Ion Cyclotron Radio Frequency (ICRF) heating of minority ion species [4]. Therefore, control of hydrogen content is strongly required to improve ICRF heating efficiency, and further to achieving high confinement mode (H-mode) long pulse plasmas, especially for EAST tokamak with high power ICRF heating.

The influence of fuel recycling on plasma performance and the control of fuel recycling is widely studied in many tokamaks, such as NSTX, JT-60U, Tore Supra, ASDEX-U, JET, EAST, and so on. NSTX results show that the edge  $T_e$  and  $T_i$  at the L–H transition is independent of the divertor recycling for a constant plasma shape, but the power threshold of L–H transition is higher with high-recycling divertor to raise the edge temperature than that of low -recycling condition [5]. R. Cesario et al. [6] considers that a low recycling during plasma start-up phase could produce high edge electron temperature, which further contributes to the build-up of high normalized  $\beta$  regimes in the H-mode, and low recycling condition is useful for enabling the LH current drive effect at reactor graded high plasma density, as well as for promoting regimes with improved confinement in large plasma volumes.

The increasing recycling during long pulse operation is mainly attributed to the increased first wall surface temperature and gradual saturation of first wall surface. During JET ITER-Like Wall (ILW) operation, released deuterium atoms or molecules from first wall surface is shown to be mainly due to strong ELM-induced particle bombardment and increasing first wall temperature [7]. The balance between particle exhausting via ELM and refueling by intra-ELM deuterium flux, together with implantation and diffusion of deuterium in near surface region, plays important role in the variation of fuel recycling. Moreover, a pronounced second peak of  $D\alpha$  radiation and divertor ion flux during JET-ILW operation is  $\sim 8$  ms later than the initial ELM crash, and probably due to desorption of implanted energetic intra-ELM deuterium ions. Results from both Alcator C-Mod [8] and ASDEX-U [9] show that fuel recycling from main chamber wall plays an important role in the global fuel recycling together with divertor recycling, and main chamber recycling is strongly related to the neutral pressure in the mid-plane, and the neutral flux is increased with plasma heating power and density. In Tore Supra long pulse operation of  $\sim 2$  min, plasma density is increased notably due to the heating of both first wall and other vessel wall far from plasmas [10], while the vessel wall far from plasmas could be baked during wall conditioning phase, and radiation heating during long pulse operation leads to strong desorption of impurities, leading to notable density increase, and the increase of density is faster with higher injected and radiated energy.

Therefore, fuel recycling must be actively controlled for long pulse plasma operation [11]. By using active cooling of plasma facing components, longer pulse operation of 6 min in Tore Supra was achieved with no wall saturation even after 3 shots with a total accumulated duration of 15 min, indicating fuel recycling and plasma density is effectively controlled by the actively cooling [12]. In contrast to Tore Supra of active cooling PFCs, hot wall operation is employed in QUEST for long pulse operation [13], because the hot wall operation reduces the fuel retention on the first wall surface, therefore it could extend the pulse length of plasma. Long pulse plasma of 1 h 55 min is achieved in QUEST with 40 kW 8.2 GHz microwave under 393 K hot wall.

However, the plasma was still terminated by the uncontrollably increased density, i.e. uncontrollable fuel recycling, even with under the hot wall operation. It indicates that hotter wall with constant temperature during plasma operation could help recycling control, but the recycling would still be increased to uncontrollable value with constant first wall temperature due to gradually saturated wall surface. JT-60U results show that [14] in reversed shear plasmas, core improved confinement is successfully isolated from high recycling and strongly radiative boundary plasmas by Internal Transport Barrier (ITB), this scenario could provide both good core plasma performance and low heat load on divertor by high radiation, and it is considered as a very promising scheme for fusion reactors.

In EAST tokamak, various wall conditionings are employed to control hydrogen content and fuel recycling, and long pulse plasmas with good performance are achieved and improved gradually with low impurity content, low hydrogen content and low fuel recycling, including first wall baking and discharge cleanings, silicon and lithium coatings, and Lithium Powder Injection (LPI) [15,16]. Long pulse H-mode plasma of 101 s is achieved in 2017 with low fuel recycling [17]. This paper is aimed to study the effective control of hydrogen content and fuel recycling for high-power long pulse plasma operations in EAST, and to provide valuable references of effective control methods for future EAST and ITER long pulse and steady state plasma operation.

Various methods on hydrogen content and fuel recycling has been employed in EAST tokamak, including first wall baking, discharge cleanings, In-Vessel Cryopumps (IVCP), first wall surface coating by silicon and lithium materials, Real-time Lithium Powder Injection (LPI). Some of the above methods have been discussed in many published papers, this paper describes the comparison on these different methods, and the paper is especially focused on, (a) the effect of IVCP, (b) detailed comparison between long-term silicon coating and lithium coating, (c) further discussion of LPI by using particle balance to quantify the global recycling coefficient, (d) fuel recycling control in over 100 s H-mode plasmas in EAST.

The paper is organized as follows: section 1 is an introduction on fuel recycling and its control on current tokamaks, section 2 describes EAST tokamak device and wall conditioning systems, section 3 shows the main results of hydrogen content and recycling control by various methods, section 4 is the realization of long pulse H-mode plasmas in EAST, and section 5 is the discussion and conclusions on the hydrogen content and fuel recycling control in EAST and future fusion devices.

## **2. EAST tokamak and wall conditioning systems**

EAST is a fully superconducting tokamak with advanced divertor configurations, the main objective of EAST experiments is to achieve long pulse and high-power plasma operation, which requires low impurity level, low fuel recycling and controlled Edge Localized Mode (ELM) plasmas. The lower divertor is made of graphite, other in-vessel components are changed to ITER-relevant metal materials since 2014, including molybdenum first wall, graphite lower divertor and tungsten upper divertor. All ITER-relevant auxiliary heating and current drive systems are equipped in EAST, in EAST 2018 campaign, the auxiliary heating systems of EAST include Neutral Beam Injection (NBI) system with co (4 MW) and counter (4 MW) injection, 140 GHz Electron Cyclotron Resonance Heating (ECRH, 2 MW), 4 MW 2.45 GHz and 6 MW 4.6 GHz Lower Hybrid Current Drive (LHCD), 6 + 6 MW Ion Cyclotron Radio Frequency (ICRF) with the frequency in 25-75 MHz [18]. 102 s L-mode long pulse plasma operations have been achieved in EAST tokamak in 2016 [19], H-mode long pulse plasmas are also achieved and extended in EAST tokamak, from 32 s in 2012 [20], to 61 s in 2016 [21] and to 101 s in

2017 [17]. Impurity control, hydrogen content control and fuel recycling control play a key role in the achievement of long pulse operation in EAST.

EAST vacuum vessel is equipped with in-vessel cryopumps for particle exhaust and recycling control in both lower and upper divertor, and each with a nominal pumping speed of  $75 \text{ m}^3/\text{s}$  for deuterium [22]. Moreover, various advanced wall conditionings are developed in EAST tokamak, which are used in different experimental phase for impurity and recycling control. (1) First wall baking using hot  $\text{N}_2$  circulation in tubes of heat sink, and the maximum temperature of first wall could be heated to  $\sim 200 \text{ }^\circ\text{C}$ . (2) Direct-Current Glow Discharge Cleaning (DC-GDC) with four independent anode and power supply, each anode with  $3 - 6 \text{ A/anode}$  and  $100 - 500 \text{ V}$  typically. (3) High Frequency Glow Discharge Cleaning (HF-GDC), by using the same anode as DC-GDC and a high frequency power supply of  $100 \text{ kHz}$ ,  $2400 \text{ V}$ ,  $10 \text{ A}$ . (4) Ion Cyclotron Radio Frequency discharge cleaning (ICRF-DC), with 2 dedicated RF antenna for ICRF-DC only, and a  $50 \text{ kW}$   $27.12/40.68\text{MHz}$  RF generator. (5) Silicon coating by using  $10\% \text{ SiD}_4 + 90\% \text{ helium}$  DC-GDC/ICRF-DC. (6) Lithium coating by evaporation with three deeply movable ovens of high temperature ( $500 - 550 \text{ }^\circ\text{C}$ ) for high coverage and assisted by helium DC-GDC/ICRF-DC, usually  $1 - 3$  hours one time, and  $\sim 10 - 45 \text{ g/coating}$ . (7) Real-time lithium powder injection (LPI) during plasma operation by using lithium dropper (developed by Princeton Plasma Physics Lab) [23].

### 3. Control of recycling and hydrogen content

#### 3.1. Baking and discharge cleanings

In EAST tokamak, long time wall conditionings are routinely used during the initial phase of a campaign, i.e. just after the sealing of all vacuum port, by using the combination of first wall baking and DC-GDC with alternate deuterium and helium. High surface temperature improves impurity desorption from first wall surface. Due to relative uniform baking of first wall, the entire first wall surface could be conditioned by baking. DC-GDC is more efficient than baking because high energy particles could be produced during DC-GDC, which bombard impurity particles adsorbed on the first wall surface, leading to the desorption of impurity particles from the first wall surface via (a) particle-induced desorption via energy transmission, (b) producing volatile by chemical reaction during bombardment, or (c) isotope-exchange.  $\text{D}_2$  DC-GDC is used to remove impurities via chemical reaction such as  $\text{H}_2\text{O}$ ,  $\text{CO}$ ,  $\text{CO}_2$  and to remove hydrogen on the surface via isotope-exchange, which is more efficient than He DC-GDC with only particle-induced deposition. However, during  $\text{D}_2$  DC-GDC, a lot of deuterium is implanted into the first wall surface, induced to strong desorption of deuterium during the main plasma operation. Therefore, alternate  $\text{D}_2/\text{He}$  DC-GDC is used during the long-time wall conditioning phase, in order to both remove impurity efficiently and reduce deuterium retention on the first wall surface.

Wall conditioning procedure in the initial phase of EAST 2015-2016 campaign is shown in Fig. 1, continuous first wall baking of up to  $\sim 200 \text{ }^\circ\text{C}$  is used and followed by  $\text{D}_2/\text{He}$  DC-GDC. Hydrogen content is gradually removed, and the partial pressure of hydrogen and water is decreased day by day as shown in Fig. 1. When the first wall baking is stopped and first wall temperature falls to room temperature, all impurity pressures are obviously reduced and much lower than that before wall conditioning except deuterium (due to intensive deuterium DC-GDC), as shown in Fig. 1(c) and Fig. 2. During the wall conditioning phase in EAST 2015-2016 campaign, the total amount of removed hydrogen is  $\sim 2$  grams, and high ultimate vacuum of  $3.6 \times 10^{-6} \text{ Pa}$  is achieved, and the total outgassing rate is decreased from  $10^{-2} \text{ Pa m}^3/\text{s}$  before baking and discharge cleanings to  $1.5 \times 10^{-4} \text{ Pa m}^3/\text{s}$ , providing a necessary clear vacuum condition for the followed physical experiments.

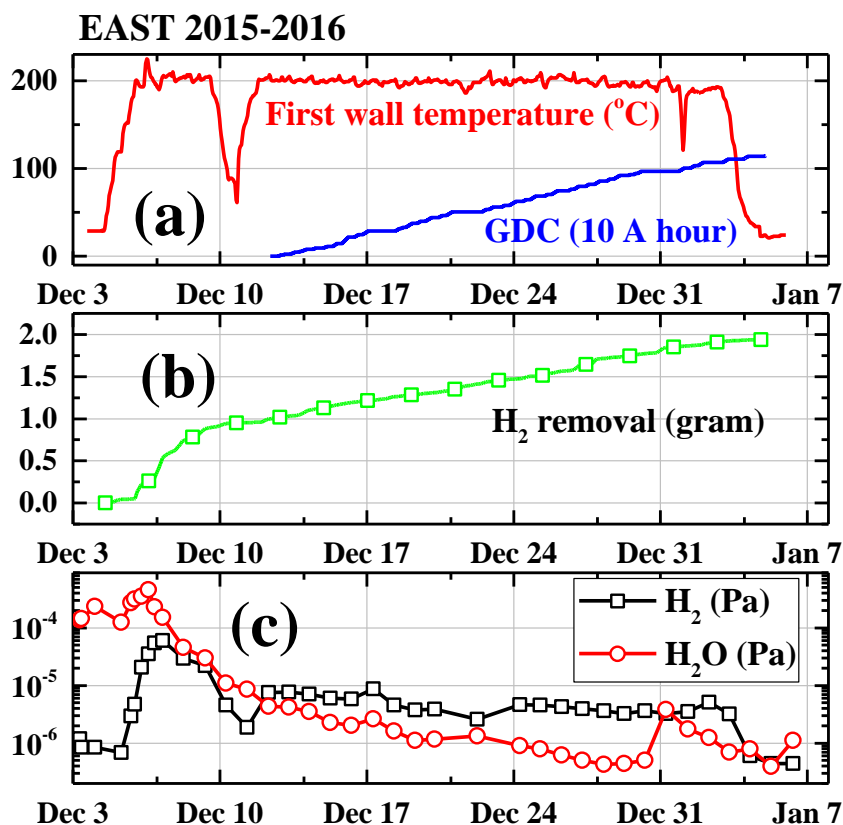


Fig. 1 Wall conditioning procedure in EAST 2015-2016 campaign, (a) first wall temperature (red line) and accumulated GDC operation duration (blue line), (b) accumulated amount of removed H<sub>2</sub> in gram, (c) partial pressures of H<sub>2</sub> (black line with  $\square$ ) and H<sub>2</sub>O (red line with  $\circ$ ).

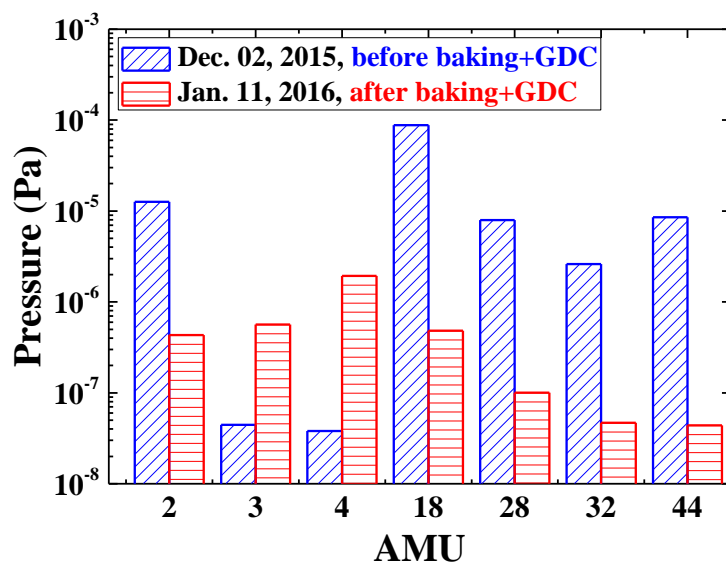


Fig. 2 Partial pressures in vacuum vessel before and after wall conditionings in EAST 2015-2016 campaign.

### 3.2 In-Vessel Cryopump

It's well known that recycling particles are firstly from hot plasma boundary, they bombard first wall surface and return to plasma boundary as neutrals, and then are ionized to fuel plasma again. In a diverted plasma, neutral pressures in divertor region is increased by this recycling process with compression due to closed construction of divertor. Moreover, plasma fueling by recycling particles should strongly depends on the neutral density around plasma boundary. The dependence of recycling

flux on neutral pressure in divertor region is studied,  $D\alpha$  emission from divertor region is used to represent the recycling flux. Experimental data are selected from EAST2018 campaign from  $\sim 90$  shots with different heating power and L/H mode in different discharge time. The results are shown in Fig. 3. It could be seen that even though the points are discrete,  $D\alpha$  emission is increased with the increase of neutral pressure in both upper and lower divertor region, which means fuel recycling could be effectively controlled by decreasing the neutral pressure in divertor region. Moreover, the results in Fig. 3 also show that both neutral pressure and recycling flux is increased with plasma heating power, i.e. fuel recycling is enhanced strongly with the increase of plasma heating power, therefore fuel recycling control must be actively controlled especially in high power operation.

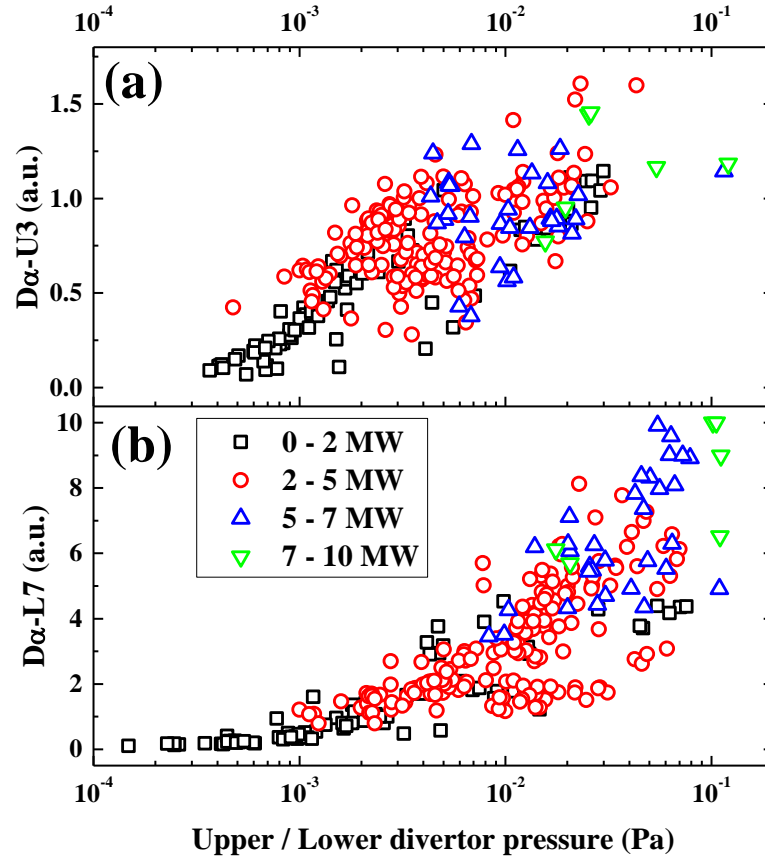


Fig. 3 Dependence of recycling flux on neutral pressure in upper (a) and lower (b) divertor region with different plasma heating power. In both (a) and (b), 0 – 2 MW is represented as red square ( $\square$ ), 2 – 5 MW red circle ( $\circ$ ), 5 – 7 MW blue upper triangle ( $\triangle$ ) and 7 – 10 MW green down triangle ( $\nabla$ ).

EAST has been equipped with In-Vessel Cryopumps (IVCP) in both upper and lower divertor region, with a total nominal pumping speed for deuterium of  $75 \text{ m}^3/\text{s} \times 2 = 150 \text{ m}^3/\text{s}$ . IVCP plays an important role in particle exhaust and fuel recycling control during diverted plasma operation, since most exhausted particles from plasmas are flowing to divertor region in diverted plasmas. The effect of IVCP effect is clearly shown in Fig. 4 by comparing two similar discharge shots with and without IVCP. The two shots, EAST #54518 and EAST #54390, are in same operation parameters: plasma current 400 kA, Lower Single Null (LSN) configuration, and Ohmic Heating (OH). There is no further gas puffing after plasma started in the two discharges as shown in Fig. 4(a).

It could be seen from Fig. 4(b-e) that, with the assist of IVCP, neutral pressure in both upper and lower divertor region is strongly decreased by a factor of  $\sim 2$ , and particle exhausting rate is increased by a factor of  $\sim 6$ , from  $\sim 5.9 \times 10^{18}$  D-atoms/s in EAST #54390 without IVCP to  $2.4 \times 10^{19}$  D-atoms/s in EAST #54518 with IVCP. Eventually,  $D\alpha$  emission is decreased by a factor of  $\sim 4$ , the plasma density is decreased from  $\sim 0.7 \times 10^{19}$  to  $0.4 \times 10^{19} \text{ m}^{-3}$ , and the global recycling coefficient

$R_{global}$ , defined by the ratio of total fueling particle flux by recycling to total particle confinement loss flux, is decreased from  $\sim 1.0$  to  $\sim 0.8$ , indicating the strong effect of recycling control of IVCP.

Because EAST #54518 is a low heating power plasma with only ohmic heating, the neutral pressure in divertor region is relatively low. In high-power heating plasma operation with several MW auxiliary heating, the neutral pressure in divertor region could be up to  $10^{-2} - 10^{-1}$  Pa range, and particle exhausting rate via IVCP is  $\sim$  up to  $10^{21} - 10^{22}$  D-atoms/s, playing a key role in fuel recycling control. Moreover, particle exhausting rate of EAST lower IVCP is much higher than that of upper one during both USN and LSN plasma configuration, probably because the lower divertor is a more closed structure than upper divertor [24].

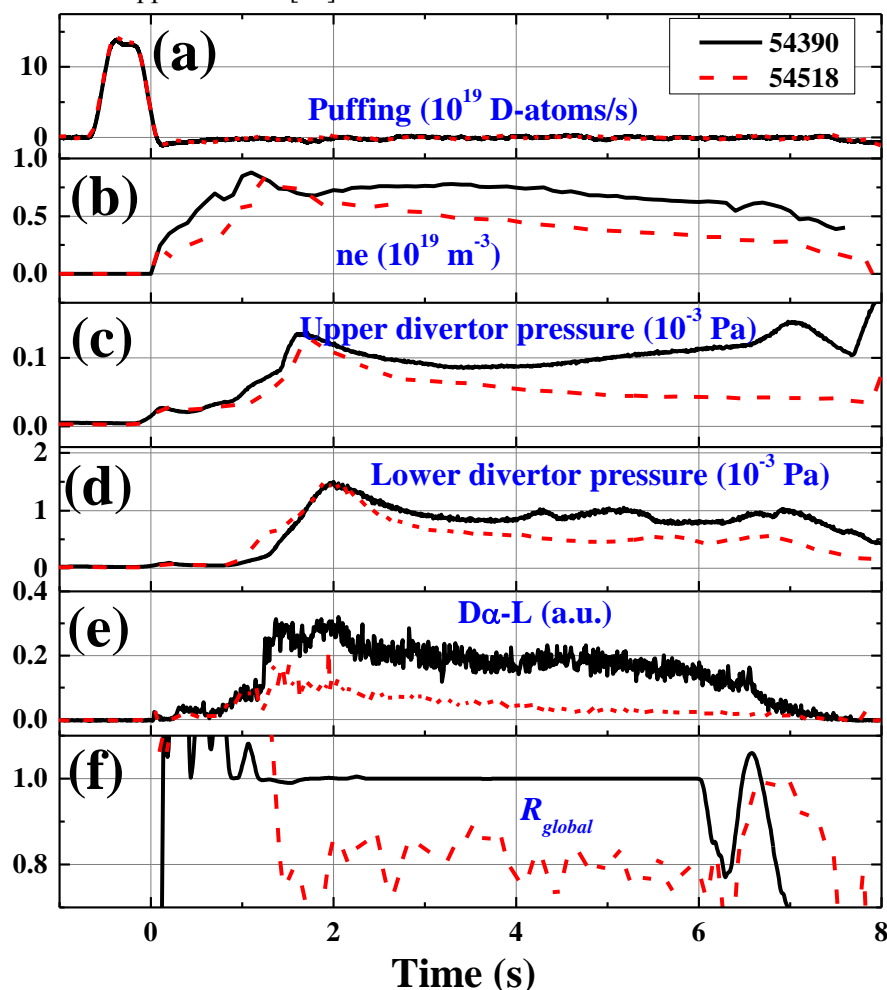


Fig. 4 Plasma parameters of EAST #54390 without IVCP (black solid line) and EAST #54518 with IVCP (red dash line), (a) gas puffing rate in  $10^{19}$  D-atoms/s, (b) plasma density in  $10^{19} \text{ m}^{-3}$ , (c) neutral pressure in upper divertor region in  $10^{-3}$  Pa, (d) neutral pressure in lower divertor region in  $10^{-3}$  Pa, (e)  $D\alpha$  emission in lower divertor region, (f) global recycling coefficient  $R_{global}$ .

### 3.3 Hydrogen control by silicon and lithium coating

Even though vacuum conditioning is notably improved, and a good ultimate pressure is achieved by using long time baking and discharge cleaning, strong impurity radiation and hydrogen recycling are still observed at the initial phase of plasma operation, which makes plasma start-up difficult and prevents the achievement of high-performance plasmas [1]. It's considered that the impurity particles ( $\text{H}_2\text{O}$ ,  $\text{CO}$ ,  $\text{CO}_2$  and so on) with low binding energy are mostly removed by long time baking and discharge cleaning, but for the impurity particles with high bonding energy, it's difficult to desorb from first wall surface because the energy transferred from baking or discharge cleaning to impurity particles with high bonding energy is not enough for desorption,

and these impurities are still kept on the surface after wall conditioning. When the main plasma operation starts, high energy particles from hot plasmas are strongly interacted with first wall surface, and impurity particles with high binding energy are desorbed from wall surface with the bombardment of main plasma particles with high energy, leading to strong impurity radiation and hydrogen recycling, which is the major problem to improve plasma performance just after wall conditioning phase.

Silicon and lithium coating with the assistant of GDC or ICRF discharge cleaning are routinely used in EAST tokamak to further depress impurity radiation and hydrogen recycling. The effects of silicon coating and lithium coating on hydrogen content and fuel recycling are well studied in EAST tokamak, and the results could be summarized as follows, (1) silicon coating could be used to reduce fuel recycling, but it's only effective in several shots, and it's difficult to decrease H/(H+D) ratio to below 20% [15], (2) lithium coating could reduce H/(H+D) ratio to 5% [15], and first H-mode plasma is achieved under lithium coating wall conditioning [25], (3) lithium coverage is improved by using more deeply inserted ovens, and effective suppression of hydrogen content, impurities and fuel recycling is achieved with improved lithium coating [26], (4) real-time lithium powder injection strongly decreases  $D\alpha$  emission in divertor region, and a reduction of 20% is achieved in divertor recycling from SOLPS simulation [27], (5) steady state ELM-free H mode is achieved together with a strong edge coherent MHD mode (ECM) by using continuous real-time injection of lithium aerosol injection [16,28], therefore transient heat load on plasma facing components and impurity accumulation is continuously depressed.

However, silicon coating is not used for a long time in Ref. [15], the effect of silicon coating on hydrogen content and fuel recycling might be improved by more silicon coatings. In EAST 2015-2016 campaign, silicon coating is almost used every day for ~ 2 months, and the effect is much better than before. As shown in Fig. 5(a), main plasmas are operated in daytime, while discharge cleaning together with silicon or lithium coating are carried out at night or early morning. Fig. 5(b) shows the ratio of H/(H+D), which is calculated by partial pressures of H<sub>2</sub>, HD and D<sub>2</sub> from residual gas analyzer by equation (1),

$$H/(H+D) = (P_{H_2} \times 2 + P_{HD}) / (P_{H_2} \times 2 + P_{HD} + P_{D_2} \times 2) \quad (1)$$

where  $P_{H_2}$ ,  $P_{HD}$  and  $P_{D_2}$  are partial pressures of H<sub>2</sub>, HD and D<sub>2</sub>, respectively. It could be seen that the ratio of H/(H+D) is decreased gradually along with SiD<sub>4</sub> coating, indicating the strong control of hydrogen from first wall surface by SiD<sub>4</sub> coating. There are two reasons of the decrease of H/(H+D), (a) hydrogen particles are continuously desorbed from first wall surface by intensive plasma wall interactions during high temperature plasma operation and GDC/ICRF discharge cleaning, and the hydrogen concentration on the wall is decreasing gradually, and (b) a thin film with silicon material is produced on the first wall surface during SiD<sub>4</sub> coating, which depresses the interactions between plasma and first wall, and therefore reduce the desorption of hydrogen.



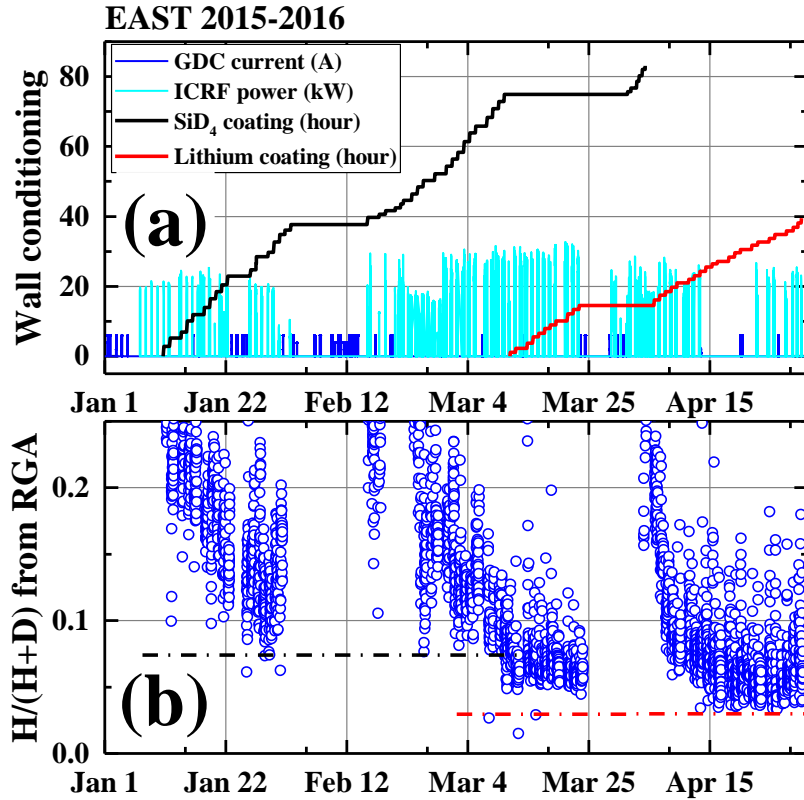


Fig. 5 (a) Wall conditioning procedure in EAST 2015-2016 campaign since plasma operation, and (b) evolution of  $H/(H+D)$  ratio from RGA along with wall conditionings, the black and red dash line represents the minimum  $H/(H+D)$  achieved by silicon coating and lithium coating, respectively.

With the reduction of  $H/(H+D)$  ratio, ICRF heating becomes efficient in high power plasma operation, as shown in Fig. 6. The shot #61609 is under silicon coating wall condition, and the main parameters of shot #61609 are, plasma current 400 kA, plasma density  $3.0 \times 10^{19} \text{ m}^{-3}$ , 2.45 GHz Lower Hybrid Wave (LHW) heating of 1.4 MW, 4.6 GHz LHW heating of 2.2 MW, and ICRF heating of 1.2 MW. It could be seen that  $D\alpha$  emission is kept constant as shown in Fig. 6(c), indicating fuel recycling is controlled well during the whole discharge. Moreover, ion temperature, measured by Tangential X-ray Crystal Spectrometer (TXCS), is increased notably from  $\sim 0.77 \text{ keV}$  to  $\sim 0.94 \text{ keV}$  with the injection of  $\sim 1.2 \text{ MW}$  ICRF power, due to the low  $H/(H+D)$  ratio.

$H/(H+D)$  ratio is increased two times due to 2 times vacuum vessel venting as shown in Fig. 5(b), first one is from Feb. 18<sup>th</sup> to 19<sup>th</sup>, and the second is from Mar. 24<sup>th</sup> to 27<sup>th</sup>. Therefore, lots of water are adsorbed again on the vacuum vessel surface during the venting time, resulting in strong outgassing of hydrogen ingredients during main plasma operation. However,  $H/(H+D)$  ratio is reduced again and to a low value of  $\sim 8\%$  with the use of  $\text{SiD}_4$  coating every day as shown in Fig. 5(b), and it's further reduced to  $\sim 5\%$  on Mar. 25, 2016 after 15 hours lithium coating, and further to  $\sim 3\%$  on Apr. 20, 2016 after  $\sim 25$  hours lithium coating. This indicates that both silicon and lithium coating are very effective on hydrogen content control, but long-term silicon coating is required, while lithium coating is more powerful and more efficient.

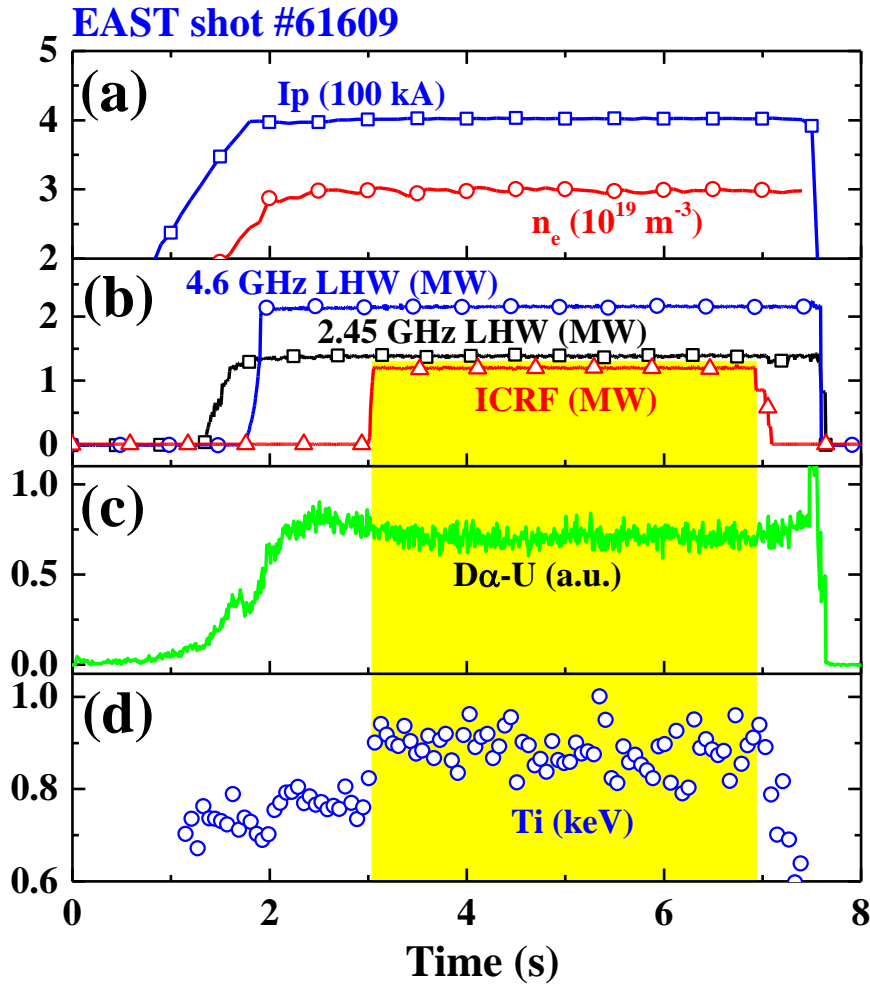


Fig. 6 High power heating plasmas under silicon coating wall, yellow region shows the ICRF heating duration, (a) plasma current (blue square) and density (red circle), (b) plasma heating power, 2.45GHz LHW (black line with  $\square$ ), 4.5 GHz LHW (blue line with  $\circ$ ), and ICRF (red line with  $\triangle$ ), (c)  $D\alpha$  emission in upper divertor region, (d) ion temperature in keV.

### 3.4 Fuel recycling control by silicon and lithium coating

As mentioned in section 3.3, fuel recycling control by lithium coating is well studied in EAST before, but deep comparison between silicon coating and lithium coating has not been carried out before, especially for silicon coating with long term. This section provides statistics data of fuel recycling under silicon coating and lithium coating wall conditions. The fuel recycling is represented by  $DaU/(n_e\tau_p)$ , where  $DaU$  is average  $D\alpha$  emission of totally 13 channels in upper divertor region, it represents the plasma fueling flux by recycling particles.  $n_e$  is line integrated plasma density in  $\text{m}^{-3}$ ,  $\tau_p$  is particle confinement time in second, which is assumed as 2 times of energy confinement time.  $n_e\tau_p$  is considered to be linear to particle flux from core plasma due to particle confinement loss. Therefore  $DaU/(n_e\tau_p)$  is theoretically linear to global recycling coefficient ( $R_{global}$ ). The average value of  $DaU/(n_e\tau_p)$  during 4 – 7 s of plasma shots are counted for statistics, and the results are shown in Fig. 7 together with normalized CIII emission by  $n_e\tau_p$  in upper divertor.

It can be seen in that fuel recycling has large variation in different discharges, not only under silicon coating wall, but also under lithium coating wall. It's because plasma operation changes with slightly different magnetic configuration and heating powers. Higher recycling behavior could be found in shots with higher plasma heating power, even though the particle confinement time is involved. Moreover, there is no sharp decrease of fuel recycling behavior after the usage

of lithium coating as shown in Fig. 7, i.e., the difference between silicon coating wall and lithium coating wall is not obvious. This also confirms that long term silicon coating provides a similar low recycling wall condition as that of lithium coating. However, the variation of fuel recycling with heating power  $> 3$  MW under lithium coating wall is smaller than that under silicon coating wall, implying the better control of fuel recycling of lithium coating than silicon coating. Moreover, CIIIU normalized by  $n_e\tau_p$  shows more obvious difference between silicon coating and lithium coating in Fig. 7(b), especially in higher power heating plasmas, indicating the very strong control of carbon impurity of lithium than that of silicon. Furthermore, the control of carbon impurity is essential for tungsten impurity suppression, therefore lithium coating is employed as a routine wall conditioning method rather than silicon coating, due to its effective and efficient control for hydrogen content, fuel recycling and impurities.

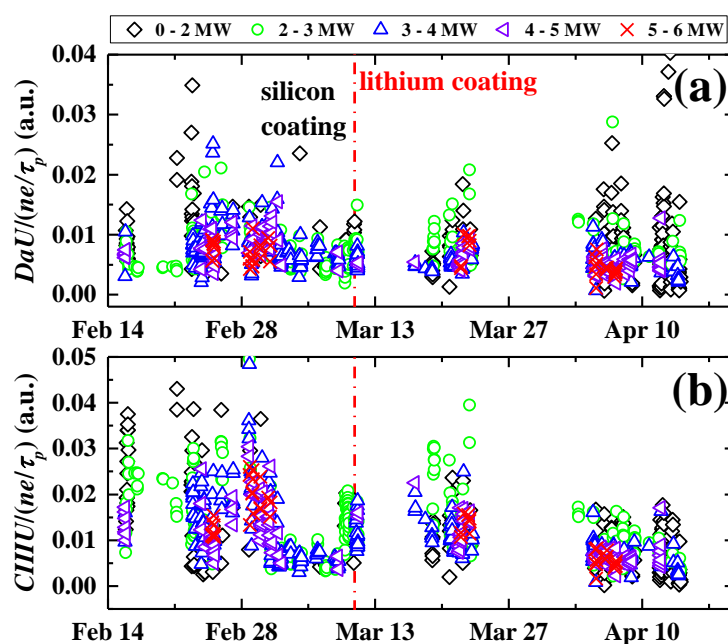


Fig. 7 Fuel recycling (a) and CIII emission (b) in upper divertor normalized by  $n_e/\tau_p$  in EAST 2015-2016 campaign with different plasma heating power, black  $\diamond$  represents 0 – 2 MW, green  $\circ$  is 2 – 3 MW, blue  $\triangle$  is 3 – 4 MW, purple  $\triangleleft$  is 4 – 5 MW, and red  $\times$  is 5 – 6 MW.

### 3.5 Real-time Lithium Powder Injection

Fuel recycling and hydrogen content is reduced to a quite low value by persistent silicon and lithium coating, and Real-time Lithium Powder Injection (LPI) is also employed to control fuel recycling and hydrogen content further during plasma operation, by using a lithium dropper system installed on the upper divertor on EAST. Fig. 8 shows two plasmas shots with same plasma operation parameters: plasma current  $\sim 500$  kA, plasma density  $\sim 2.8 \times 10^{19} \text{ m}^{-3}$ , Upper Single Null (USN), 2.45 GHz LHW 0.5 MW, 4.6 GHz LHW 2.0 MW, and  $\sim 0.5 - 0.6$  MW ICRF heating only from 7.0 - 9.0 s, gas puffing  $\sim 9.2 \times 10^{20}$  D-atoms/s from 1.0 – 8.0 s. The two shots are EAST #70099 with real-time LPI and EAST #70096 without LPI, and they have been investigated in detail by J.M. Canik et al. [27], on fuel recycling in via the decrease of  $D\alpha$  emission and particle flux on divertor surface, and SOLPS simulation results show that the global recycling coefficient ( $R_{global}$ ) is decreased by  $\sim 20\%$  by LPI. It could be seen from Fig. 8(b-c) that the total amount of SMBI particles is 1.8 times higher in LPI shot than that without LPI, and the number of pumped particles by first wall and lithium film is also 1.5 times higher than that without LPI. Moreover, Li-II emission in upper divertor is strongly increased and  $D\alpha$

emission is notably decreased and the global recycling coefficient indicating strong control of fuel recycling by real-time LPI.

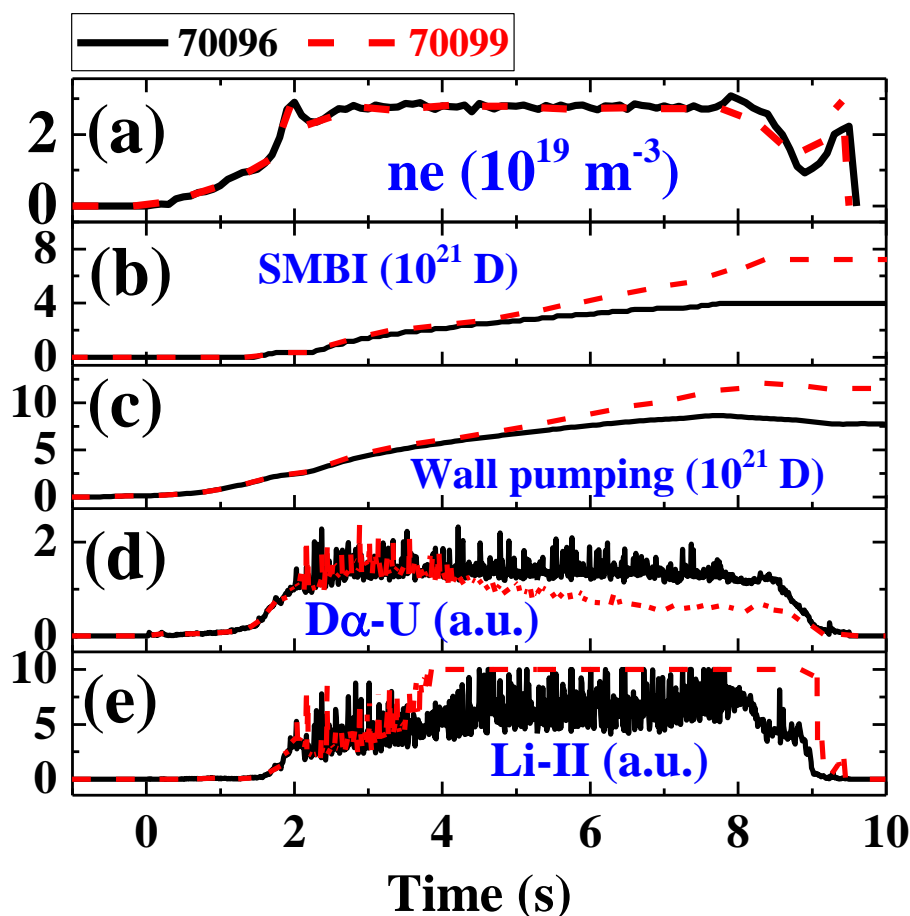


Fig. 8 Fuel recycling control by real-time LPI in EAST # 70099 (red dash line) compared with EAST #70096 without lithium injection (black solid line), (a) plasma density in  $10^{19} \text{ m}^{-3}$ , (b) accumulated amount of SMBI in  $10^{21} \text{ D}$ -atoms, (c) total amount of particles pumped by first wall and lithium film in  $10^{21} \text{ D}$ -atoms, (d)  $\text{D}\alpha$  emission in upper divertor region, and (e)  $\text{Li-II}$  emission in upper divertor region.

A further investigation on the two shots above are carried out. Quantitatively results on particle flux and fuel recycling are evaluated, by using particle balance with some assumptions [24], and the results are shown in Fig. 9. The divertor recycling coefficient  $R_{div}$  in Fig. 9(d) is defined by recycling particle flux from divertor plate normalized by total particle flux to divertor plate including both upper and lower divertor. Fueling efficiency of divertor recycling particle  $\alpha_{div}$  in Fig. 9(e) is defined by the ratio of recycling particle flux entering main plasma region to the total recycling particle flux from divertor region. It could be seen in Fig. 9(a-c) that the particle confinement loss and particle flux to upper and lower divertor are all similar with and without real-time LPI, because the plasma density and confinement are same in the two shots. Divertor recycling coefficient  $R_{div}$  is lower than 1, but  $R_{div}$  in real-time LPI shot is obviously lower than that without lithium injection. The fueling efficiency of recycling flux is in the range of  $10^{-3}$ , and it's also decreased by real-time LPI as shown in Fig. 9(e). The decrease of divertor recycling coefficient  $R_{div}$  and recycling fueling efficiency  $\alpha_{div}$  leads to a reduction of 5 - 10% on the plasma fueling flux by recycling particles as shown in Fig. 9(f), induced by real-time LPI. It's probably because the plasma temperature on divertor plate is decreased by LPI [29], leading to a reduced energy of recycling particles and decreased the fueling efficiency of recycling flux.  $R_{global}$  evaluated by particle balance analysis is decreased from  $\sim 0.94$  to  $0.82$  by real-time LPI

as shown in Fig. 9(g), the value of  $R_{global}$  decrement is  $\sim 0.12$ , it's close to SOLPS simulation result of 20% [27], indicating the good agreement between experiments and simulation on the effective control of fuel recycling by LPI.

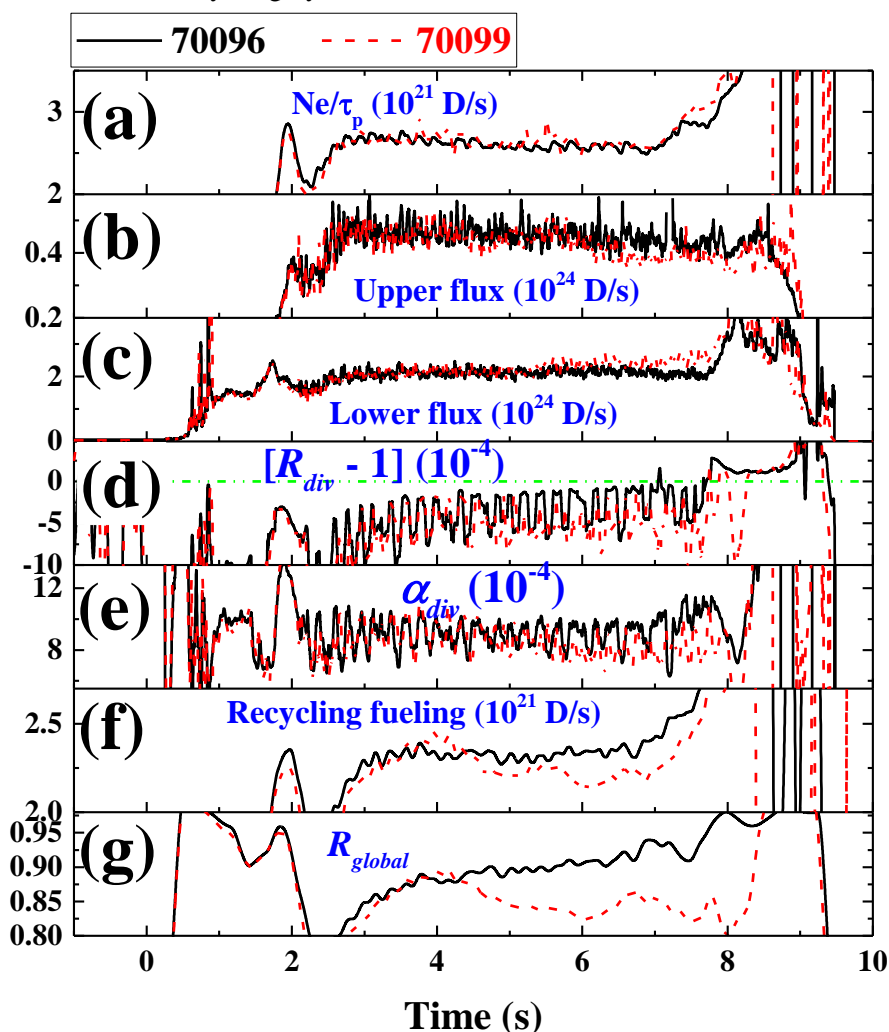


Fig. 9 Particle balance analysis results of EAST #70096 (black solid line) and EAST # 70099 (red dash line), (a) particle confinement loss in  $10^{21}$  D/s, (b) upper divertor particle flux measured by Langmuir probe array in  $10^{24}$  D/s, (c) lower divertor particle flux measured by Langmuir probe array in  $10^{24}$  D/s, (d) average recycling coefficient ( $R_{div}$ ) of upper and lower divertor, the value is subtracted by 1 in order to be read clearly because  $R_{div}$  is very close to 1, the horizontal green dash dot line is the value of zero, (e) fueling efficiency of divertor recycling particles, (f) plasma fueling flux by divertor recycling particles in  $10^{21}$  D/s, and (g) global recycling coefficient  $R_{global}$ .

#### 4. Realization of long pulse H-mode plasmas in EAST

##### 4.1 Long pulse L-mode plasmas under silicon coating wall

In EAST 2016 campaign, long-term silicon coating ( $\text{SiD}_4$ ) wall conditioning is firstly used rather than lithium coating, and hydrogen content is decreasing along with successive silicon coatings, as shown in Fig. 5(b). 102 s long pulse L-mode plasmas with a core electron temperature of  $>5$  keV is obtained in EAST #59892 under silicon coating wall conditioning with an accumulated silicon coating duration of  $\sim 38$  hours. The main parameters of EAST #59892 are: plasma current 400 kA, plasma density  $1.5 \times 10^{19} \text{ m}^{-3}$ , LSN, hybrid heating with 0.5 MW 2.45 GHz LHW, 1.4 MW 4.6 GHz LHW, 0.4 MW 170 GHz ECRH and 0.4 MW modulated Neutral Beam Injection. Even though the plasmas are stably maintained for 102 s, plasma density is increased slight since  $\sim 80$  s. First wall temperature measured by thermocouples is increased slightly from 24  $^{\circ}\text{C}$  to 128  $^{\circ}\text{C}$  at the end of

discharge,  $D\alpha$  emission is also increased slightly with first wall temperature, as shown in Fig. 10(c), indicating that fuel recycling is increased along with the first wall temperature. The wall pumping rate represents the same result on recycling, it's decreased and becomes negative since  $\sim 80$  s, and plasma density is also increased since the same time without external gas injection, which means that fuel recycling is uncontrollably increased since  $\sim 80$  s. This result indicates that silicon coating effect on fuel recycling control is effective but limited for long pulse operation, and other methods should be also employed for further control on fuel recycling in long pulse plasma operation with high performance.

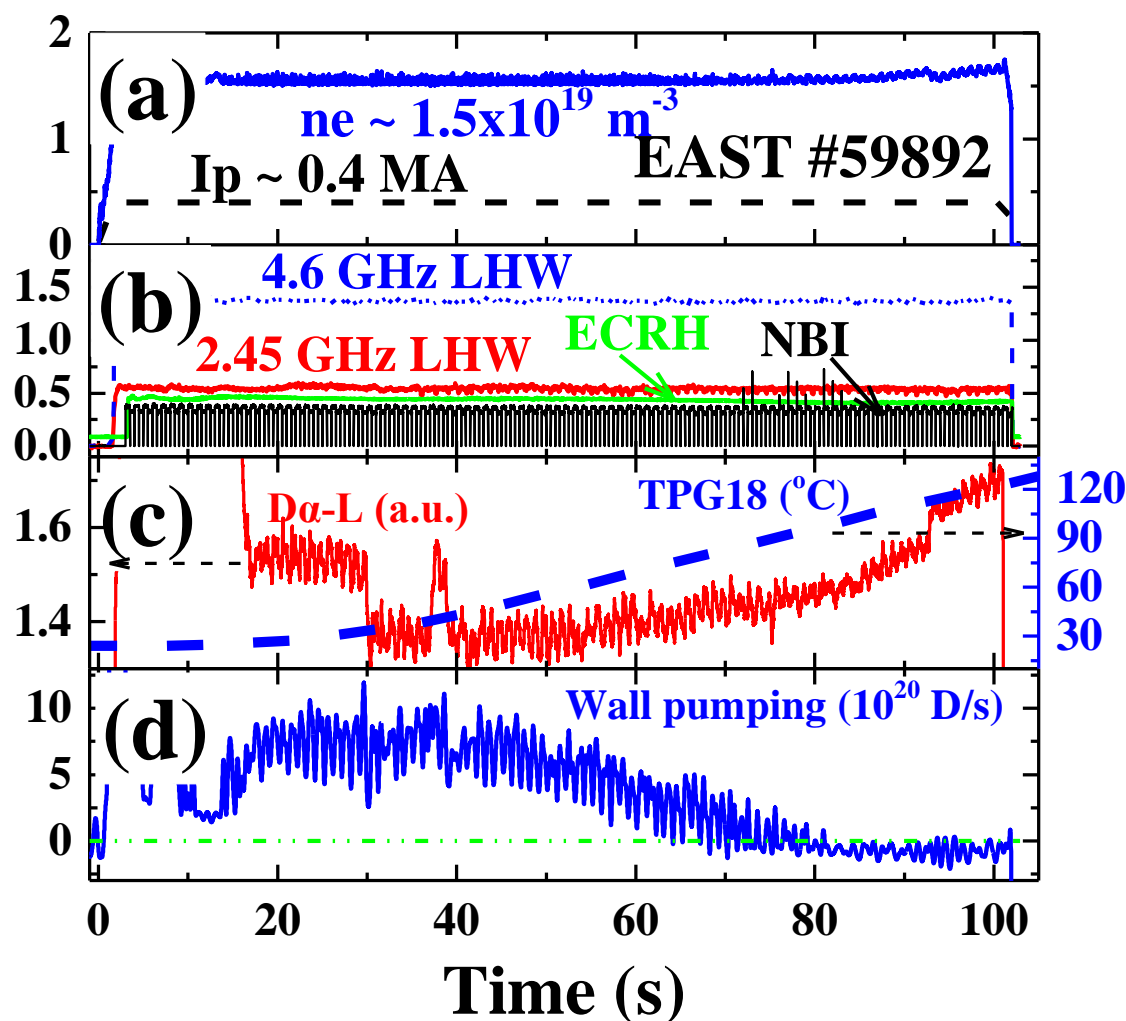


Fig. 10 Long pulse L-mode of EAST #59892, (a) plasma current (black dash line) and plasma density (solid blue line), (b) auxiliary heating of 2.45 GHz LHW (solid red line), 4.6 GHz LHW (dash blue line), ECRH (solid green line) and modulated NBI (solid black line), (c)  $D\alpha$  emission (red solid line) and first wall temperature (blue dash line) on inner lower divertor plate measured by thermocouple, and (d) wall pumping rate (blue line), dash green line represents zero, i.e. saturated wall condition.

#### 4.2 Extension of long pulse H-mode plasmas

Long pulse high-performance plasma operation is one of missions of EAST tokamak. Lots of efforts have been made on EAST long pulse H-mode operation in recent EAST campaigns, including long time first wall baking and discharge cleanings, intensive lithium coating and real-time LPI, and so on. The duration of achieved long pulse H-mode plasmas are extended from 32 s in 2012 to 61 s in 2016 and to 101 s in 2017 as shown in Fig. 11. The 32 s H-mode plasma (EAST #41195) is Double Null (DN) divertor configuration with  $H_{98} \sim 0.8$ , plasma current 280 kW, plasma density (2.0 – 2.5)

$\times 10^{19} \text{ m}^{-3}$ , and 2.7 MW auxiliary heating by LHW and ICRF under lithium coating wall condition. It could be seen that  $D\alpha$  emission is increased since  $\sim 10$  s in EAST #41195, and the plasma density is also increased slightly from  $\sim 2.0 \times 10^{19}$  to  $\sim 2.5 \times 10^{19} \text{ m}^{-3}$ , indicating increased fuel recycling along with discharge. 61 s long pulse H-mode of EAST #67341 is USN configuration (upper tungsten divertor and lower graphite divertor) with  $H_{98} \sim 1.1$ , it's also operated under lithium coating wall condition together with operation of both lower and upper divertor in-vessel cryopumps. As shown in Fig. 11(b),  $D\alpha$  emission is almost constant and even decreased at the end of this discharge, indicating a good control on fuel recycling. The increase of plasma density of EAST #67341 at the end of discharge ( $> 48$  s) is due to enhancement of carbon impurity, which results from a hot-spot on lower divertor. In the 101 s H-mode discharge of EAST #73999 with also USN configuration with  $H_{98} \sim 1.1$ ,  $D\alpha$  emission is slightly decreased along with discharge, and plasma density is constant between 0 - 60 s, and then decreased a little until the termination of discharge, i.e. fuel recycling is well controlled.

Even though the three discharges are in different divertor configuration (DN and USN) and different plasma density variation, it could be seen that  $D\alpha$  emission has strongly related to Li-II emission. With the increase of Li-II emission in the later phase of long pulse operation of EAST #67341 and #73999,  $D\alpha$  emission is decreased obviously along with the increase of lithium emission, indicating that lithium plays vital roles on fuel recycling control. Moreover, the increase of Li-II emission is probably due to the increasing of first wall temperature, leading to evaporation or desorption of lithium films which has been coated on the first wall surface before, and then the edge deuterium recycling is reduced by the increased lithium flux.

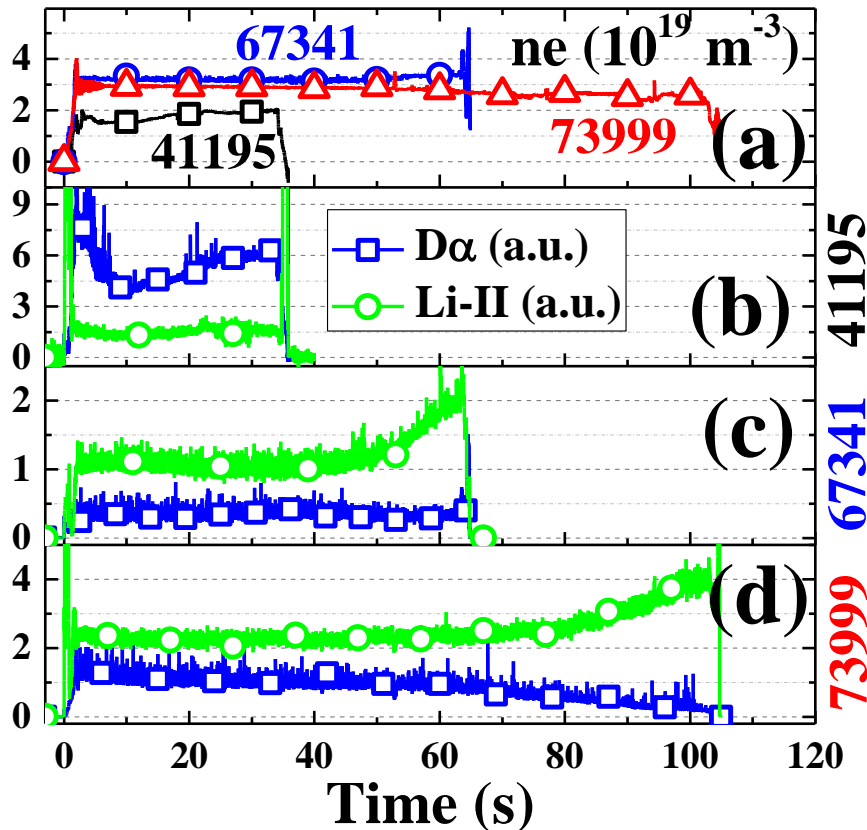


Fig. 11 Long pulse H-mode discharges in EAST, (a) plasma density of EAST #41195 (black line with  $\square$ ), EAST #67341 (blue line with  $\circ$ ) and EAST #73999 (red line with  $\triangle$ ), (b), (c) and (d) are  $D\alpha$  emission (blue line with  $\square$ ) and Li-II emission (green line with  $\circ$ ) of three shots, respectively.

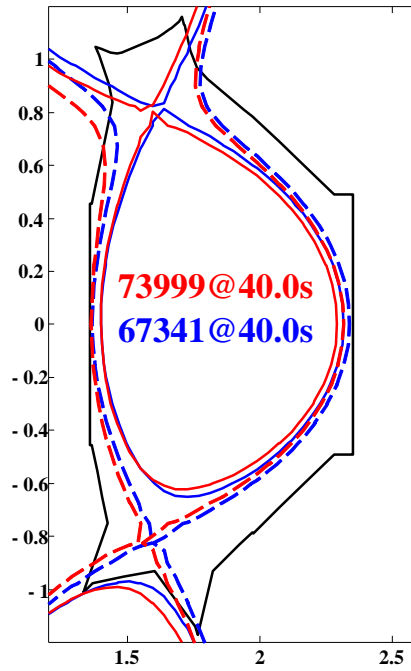


Fig. 12 Magnetic configuration of EAST #67341 (blue line) and EAST #73999 (red line) at 40.0s, plasmas move to high field side further in EAST #73999, and strike-point on outboard of lower divertor in EAST #67341 (blue dash line) is moved to dome region in EAST #73999 (red dash line).

#### 4.3 Avoidance of hotspot on lower graphite divertor

Hotspots on the lower divertor surface is one of major problems during the operation of EAST #67341, particle flux on lower divertor surface as shown in Fig. 13(f) is increased by a factor of  $\sim 1.5$  since  $\sim 25$  s in EAST #67341 due to the enhanced hotspot, and the neutral pressure in lower divertor as shown in Fig. 13(e) is also increased together with the particle flux. The particle flux and neutral pressure in lower divertor is further increased again since  $\sim 50$  s in EAST #67341, leading to an increasing particle recycling (including both deuterium recycling and impurity recycling). In order to avoid hotspot on lower graphite divertor during long pulse H-mode operation like EAST #67341, plasmas are moved to high field side further in EAST #73999 than that in EAST #67341, the strike-point on outboard of lower divertor in EAST #67341 is moved to dome region in EAST #73999 as shown in Fig. 12.

The  $dR_{sep}$  (the radial distance between the upper divertor separatrix and the lower divertor separatrix at the outboard midplane [30]) is increased from  $\sim 2.0$  cm in EAST #73999 to  $\sim 2.4$  cm in EAST #67341 as shown in Fig. 13(a), no hotspot appears on outboard of lower divertor in EAST #73999, which was a major problem during long pulse operation of EAST #67341. The particle confinement loss is similar in the two shots as shown in Fig. 13(b). In EAST #73999 with higher  $dR_{sep}$  than that in EAST #67341, particle flux on lower divertor is reduced by a factor of  $\sim 4$ , and neutral pressure in lower divertor is also decreased, and no hotspot appears during the whole discharge.

Moreover, the particle flux on upper divertor is only  $\sim 1.2$  times higher in EAST #73999 than that in EAST #67341. The neutral pressure on upper divertor of EAST #73999 is  $\sim 2.4$  times higher than that of EAST #67341, but it should be noted that the partial pressure in upper divertor region in the two shots are both one order lower than that in lower divertor region, which means that the increase of neutral pressure on upper divertor has only a little effect on the particle recycling. Lower divertor is the main channel for particle exhausting for both EAST #67341 and #73999 even with USN configuration, which is probably due to different divertor structure and material for lower and



upper divertor [24]. The global recycling coefficient as shown in Fig. 13(g) shows clearly that the particle recycling in EAST #73999 is lower than that in EAST #67341. Therefore, moving plasma to high field side is a good method to avoid hotspot on lower divertor and to control particle recycling efficiently.

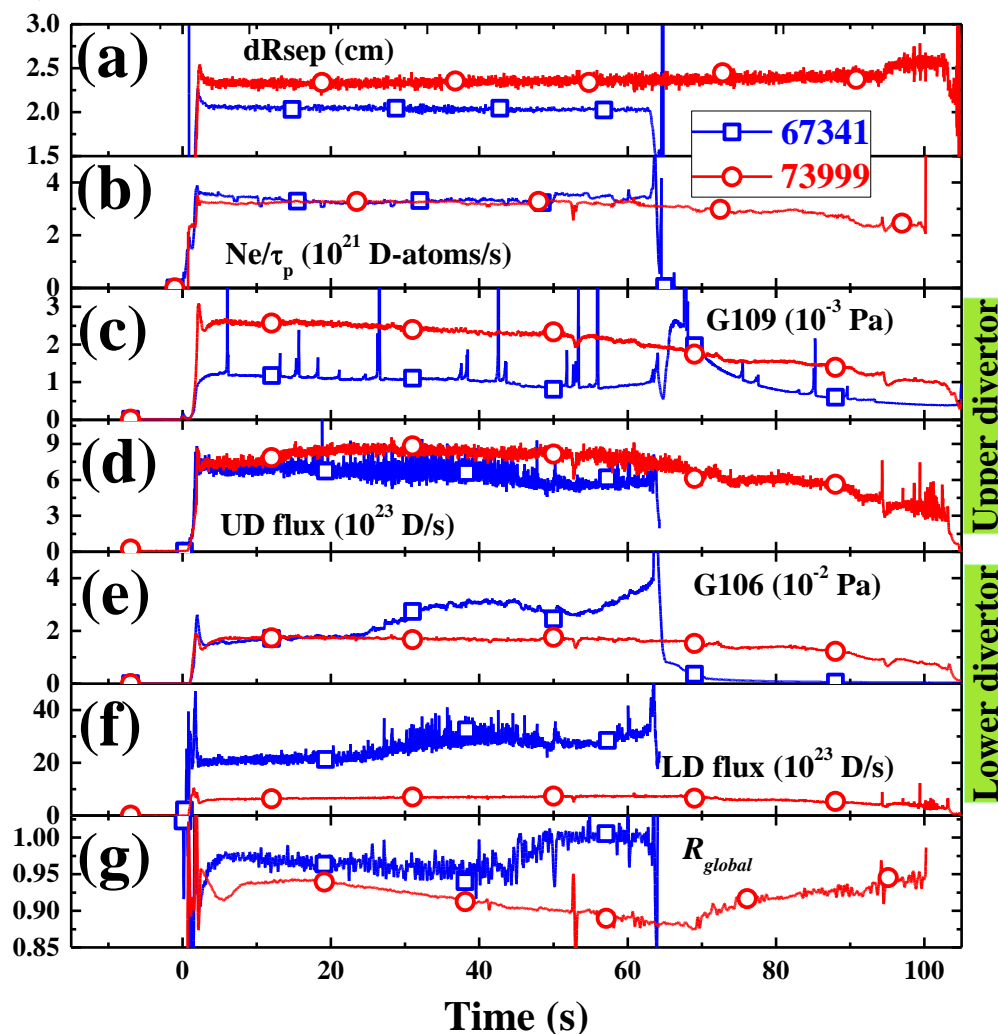


Fig. 13 Improved fuel recycling control by moving plasmas to high field side in EAST #73999 (red line with  $\circ$ ) compared to EAST #67341 (blue line with  $\square$ ), (a)  $dR_{sep}$  in cm, (b) particle confinement loss (plasma inventory divided by particle confinement time) in  $10^{21}$  D-atoms/s, (c) neutral pressure in upper divertor region, (d) particle flux on upper divertor surface measured by Langmuir probes, (e) neutral pressure in lower divertor region, (f) particle flux on lower divertor surface measured by Langmuir probes, (g) global recycling coefficient.

## 5. Discussion and conclusions

Various methods for hydrogen content and recycling control are studied in EAST tokamak for high-power long pulse plasma operations. The experimental results show that long time first wall baking and discharge cleaning remove impurities effectively from the first wall surface. The total outgassing rate from first wall is decreased from  $10^{-2}$  Pa  $m^3/s$  to  $1.5 \times 10^{-4}$  Pa  $m^3/s$ , providing a necessary clean wall condition with a high ultimate vacuum of  $3.6 \times 10^{-6}$  Pa for plasma operation. However, the energy transferred from baking or discharge cleaning to impurity particles with high bonding energy to surface is not enough for their desorption, and these impurity particles are released during main plasma operation due to particle impacting with much higher energy than that in baking or discharge cleaning. First wall coating by using silicon and lithium materials are more effective than baking and discharge cleanings for hydrogen content and fuel recycling

control.

The coated film with silicon and lithium materials on first wall surface not only suppresses the interactions between plasmas and original first wall surface, but also actively control hydrogen content and other impurities due to the strong adsorption characteristics of silicon and lithium film. Therefore, the hydrogen content and recycling are controlled effectively by silicon and lithium coating. H/(H+D) ratio is decreased gradually to  $\sim 8\%$  with intensive silicon coating, and it's further reduced to  $3\%$  by lithium coatings with an accumulated duration of  $\sim 25$  hours. Lithium coating is more effective and efficient on hydrogen isotope control than silicon coating because, (a) lithium material has stronger adsorption capability for hydrogen isotopes than that of silicon one, and (b) additional deuterium is introduced during silicon coating with  $\text{SiD}_4$ . Therefore, lithium coating is routinely used in EAST tokamak to achieve a low hydrogen content and low fuel recycling wall condition.

In-Vessel Cryopumps (IVCP) in both lower and upper divertor region have a total nominal pumping speed of  $150 \text{ m}^3/\text{s}$  for deuterium, which decreases the neutral pressure in divertor region by a factor of  $\sim 2$  and decrease  $R_{global}$  from  $\sim 1.0$  to  $\sim 0.8$  during OH plasmas. IVCPs provide a high particle exhausting rate of  $10^{20}$ -  $10^{21}$  D-atoms/s in high-power plasma operations, and control fuel recycling effectively by reducing the neutral pressures in divertor region. Real-time Lithium Powder Injection is a novel and real-time method for recycling control, which reduces  $R_{global}$  from by 0.94 to 0.82 under lithium coating wall condition. Because LPI decreases the plasma temperature on divertor plate and reduces the energy of recycling particles, therefore the plasma fueling by recycling flux is reduced by LPI.

By the combination an optimization of the above methods, first H-mode plasma with only ICRF heating of  $\sim 1.5$  MW is obtained in EAST 2012 campaign with low H/(H+D) ratio of  $\sim 10$ - $15\%$  under lithium coating. 102 s plasmas with high power heating and  $> 5$  keV core electron temperature is obtained under only silicon coating wall condition. Long pulse H-mode plasmas with high performance are extended gradually in EAST, from 32 s with 2.7 MW and  $H_{98} \sim 0.8$  in 2012, to 61 s with 3.6 MW  $H_{98} \sim 1.1$  in 2016, and to 101 s with 3.0 MW and  $H_{98} \sim 1.1$  in 2017. In all these long pulse discharges, fuel recycling is well controlled and even decreased gradually with discharge especially at the later phase of discharges, due to increased lithium emission induced by increased first wall temperature and enhanced evaporation of lithium from surface. Hotspots on lower divertor plate is also successfully avoided by moving plasmas to high field side, and therefore the strike-point on outboard of lower divertor is moved to dome region.

In conclusion, hydrogen content and fuel recycling are well controlled in EAST tokamak by combined various methods. Long time first wall baking and discharge cleaning in EAST provides necessary clean vacuum environment for plasma operation. First coating with silicon and lithium is more powerful than baking and discharge cleanings for hydrogen content and fuel recycling control, and lithium coating is more effective and efficient than silicon coating. IVCPs efficiently reduce the neutral pressures in divertor region and control fuel recycling. LPI is a real-time method to further reduce fuel recycling under lithium coating wall condition. 101 s long pulse H-mode plasmas with  $\sim 3.0$  MW auxiliary heating and  $H_{98} \sim 1.1$  is achieved in EAST 2017 campaign, with low hydrogen content and low fuel recycling and without any hotspots on divertor plates. These results provide valuable references on hydrogen content and fuel recycling control for longer pulse H-mode plasma of up to 400 – 1000 s with high-power heating in EAST and future fusion device such as ITER.

## 6. Acknowledgements

This research is supported by National Nature Science Foundation of China (11605237, 11625524, 11605236, 11605246, 11775261) and National Key Research and Development Program of China

(2017YFA0402500, 2017YFE0301100).

- [1] G. Federici, *et al.*, *Nucl. Fusion* **41** (2001) 1967-2137
- [2] S. Brezinsek, *et al.*, *Phys. Scr.* **T167** (2016) 014076
- [3] R. Majeski, *et al.*, *Phys. Rev. Lett.* **97** (2006) 075002
- [4] E. Lerche, *et al.*, *Nucl. Fusion* **54** (2014) 073006
- [5] D.J. Battaglia, *et al.*, *Nucl. Fusion* **53** (2013) 113032
- [6] R. Cesario, *et al.*, *Plasma Phys. Control. Fusion* **55** (2013) 045005
- [7] S. Brezinsek, *et al.*, *Phys. Scr.* **T167** (2016) 014076
- [8] B. Lipschultz, *et al.*, *Plasma Phys. Control. Fusion* **44** (2002) 309
- [9] K. McCormick, *et al.*, *J. Nucl. Mater.* **390-391** (2009) 465-469
- [10] C. Grisolia, *et al.*, *J. Nucl. Mater.* **266-269** (1999) 146-152
- [11] H.Y. Guo, *et al.*, *Nucl. Fusion* **54** (2014) 013002
- [12] M. Chatelier, *et al.*, *Nucl. Fusion* **47** (2007) S579-S589
- [13] K. Hanada, *et al.*, *Nucl. Fusion* **57** (2017) 126061
- [14] K. Itami, *et al.*, *Phys. Rev. Lett.* **78** (1997) 1267-1270
- [15] G Z Zuo *et al.*, *Plasma Phys. Control. Fusion* **54** (2012) 015014
- [16] J.S. Hu, *et al.*, *Phys. Rev. Lett.* **114** (2015) 055001
- [17] B.N. Wan, *et al.*, *27<sup>th</sup> IAEA Fusion Energy Conference*, Gujarat, India, Oct. 22-27, 2018
- [18] B.N. Wan, *et al.*, *Nucl. Fusion* **57** (2017) 102019
- [19] J.P. Qian, *et al.*, *Plasma Sci. Technol.* **18** (2016) 457-459
- [20] B. N. Wan, *et al.*, *Nucl. Fusion* **53** (2013) 104006
- [21] X.Z. Gong, *et al.*, *Plasma Sci. Technol.* **19** (2017) 032001
- [22] Q.S. Hu, *et al.*, *J. Nucl. Mater.* **415** (2011) S395-S399
- [23] D.K. Mansfield, *et al.*, *Fusion Eng. Des.* **85** (2010) 890
- [24] Y.W. Yu, *et al.*, *Phys. Scr.* **T170** (2017) 014070
- [25] G.S. Xu, *et al.*, *Nucl. Fusion* **51** (2011) 072001
- [26] Z. Sun, *et al.*, *Fusion Eng. Des.* **89** (2014) 2886-2893
- [27] J.M. Canik, *et al.*, *IEEE Transactions on Plasma Science* **46** (2018) 1081-1085
- [28] J.S. Hu, *et al.*, *Fusion Eng. Des.* **89** (2014) 2875-2885
- [29] W. Xu, *et al.*, *Fusion Eng. Des.* **137** (2018) 202-208
- [30] T.W. Petrie, *et al.*, *J. Nucl. Mater.* **290-293** (2001) 935-939